



## Characterization and coagulation–flocculation performance of a composite coagulant: poly-ferric-aluminum-silicate-sulfate

Wei Chen<sup>a</sup>, Huaili Zheng<sup>a,\*</sup>, Jun Zhai<sup>a</sup>, Yili Wang<sup>b</sup>, Wenwen Xue<sup>a</sup>, Xiaomin Tang<sup>a</sup>, Zhengang Zhang<sup>a</sup>, Yongjun Sun<sup>a</sup>

<sup>a</sup>Key Laboratory of the Three Gorges Reservoir Region's Eco-Environment, State Ministry of Education, Chongqing University, Chongqing 400045, China, Tel. +86 23 65120827; Fax: +86 23 65120827; email: zhl@edu.cqu.cn (H. Zheng)

<sup>b</sup>College of Environmental Science and Engineering, Research Center for Water Pollution Source Control and Eco-Remediation, Beijing Forestry University, Beijing 100083, China

Received 14 May 2014; Accepted 4 August 2014

### ABSTRACT

Composite coagulant has received widespread attention and research for its excellent coagulation performance in recent years. In this study, a new composite coagulant poly-ferric-aluminum-silicate-sulfate was synthesized using water glass,  $\text{FeSO}_4 \cdot 7\text{H}_2\text{O}$ ,  $\text{Al}_2(\text{SO}_4)_3 \cdot 18\text{H}_2\text{O}$ , and  $\text{NaClO}_3$ , their structures and morphologies were characterized and compared by X-ray diffraction, infrared spectra, and scanning electron microscopy. In addition, to obtain the optimum synthetic conditions resulting in the maximum turbidity removal efficiency, single-factor method was used to examine the parameters such as  $\text{Si}/[\text{Al}+\text{Fe}]$ ,  $\text{Al}/\text{Fe}$ , and aging time by municipal wastewater treatment. The coagulation–flocculation process showed that chemical oxygen demand and turbidity removal efficiency could achieve 77 and 99.4%, respectively, when the optimum synthesis conditions were  $\text{Si}/[\text{Al}+\text{Fe}]$ ,  $\text{Al}/\text{Fe}$ ,  $\text{OH}/[\text{Al}+\text{Fe}]$ , aging time, and reaction temperature of 0.4:1, 3:7, 0.3, 24 h, and 80°C, respectively. In addition, when the  $\text{Si}/[\text{Al}+\text{Fe}]$  of coagulant was 0.2 and 0.4, the coagulant produced lower sludge volume. The result showed that PFASS exhibit superior flocculation effect, and the main mechanisms in reducing the surface charge of colloids are neutralization and adsorption/bridging coagulation–flocculation.

*Keywords:* Composite coagulant; Poly-ferric-aluminum-silicate-sulfate; Turbidity removal; Characterization

### 1. Introduction

Environment problem caused by water pollution arouses widespread concern in society. The conventional water/wastewater treatment technique mainly consists of activated carbon adsorption, membrane filtration, physicochemical coagulation–flocculation, and biological treatment [1–3]. Water/wastewater usually

remains stable and cannot be purified by itself for charge repulsion, which is caused by the presence of micro-colloidal or suspended particles in water. The chemical coagulation–flocculation can remove the micro-colloidal or suspended particles effectively by the process of adsorption–charge neutralization, adsorption–bridge, sweep flocculation [4,5]. The coagulants can usually be divided into inorganic, organic, and composite coagulants. While, the high cost and

\*Corresponding author.

the monomer toxicity of organic coagulants have inhibited its use in the drinking water treatment [6]. Inorganic coagulants are widely used in water/wastewater treatment for the advantages of low price, convenient to use, high effluent quality, etc.

The currently used inorganic coagulant is primarily Al-based coagulants, Fe-based coagulants, and metal-based composite coagulants. Al-based coagulants and Fe-based coagulants have their own merits, whereas their shortcomings are inevitable. For aluminum coagulants, residual concentration of Al in the treated water may result in a high-potential harmful impact on human health, and the flocs form by aluminum coagulants are brittle, loose [7]. While ferric coagulant's shortcoming is obvious, corrosive, high chromaticity of effluent, e.g. compared to traditional Al or Fe coagulant, the composite coagulants usually carry a high cationic charge, which result in high charge neutralization ability and high coagulation–flocculation efficiency, for these reasons, composite coagulants have received widespread attention and application in recent years [5,8,9]. Cationic inorganic composite materials used in coagulation/flocculation of wastewater are materials refer to  $\text{Al}_2(\text{SO}_4)_3$ ,  $\text{Fe}_2(\text{SO}_4)_3$ ,  $\text{Al}_2\text{Cl}_3$ ,  $\text{Fe}_2\text{Cl}_3$ ,  $\text{ZnSO}_4$ ,  $\text{ZrO}_2$ , while anionic refer to  $\text{NaSiO}_3$ ,  $\text{H}_3\text{PO}_4$ ,  $\text{NaH}_2\text{PO}_4$ ,  $\text{Na}_2\text{HPO}_4$ , e.g. They emerged structurally hybridized, chemically bound hybridized, or functionally hybridized to form a bigger molecular structure as well as to enhance the aggregating capacity. Yubin Zeng, Junboun Park synthesized a novel coagulant by introducing Si ions in zinc sulfate to produce composite coagulant PZSS, beaker experiment showed that PZSS performed better coagulation–flocculation efficiency than PFS in removing turbidity, chemical oxygen demand (COD), and SS [9]. Bao-Yu Gao et al. prepared PASiC by combining PAC with polysilicic acid (PSi), the experiments showed that with the increasing in  $\gamma$  value, the efficiency of PASiC increased, compared to PAC, PASiC performed better removing efficiently in algae, turbidity, oil, COD, and TP under the laboratory conditions [10]. Guocheng Zhu et al. studied the polymeric aluminum ferric sulfate as a modified coagulation reagents for treatment of wastewater, they obtained the optimum synthetic conditions through response surface methodology, and the work suggested that the main mechanism in reducing the surface charge of colloid in wastewater is adsorption/bridging coagulation–flocculation mechanisms [5]. Sun [11], Li [12] prepared poly-ferric-aluminum-silicate-sulfate from fly ash, pyrite slag, and wasted sulfuric acid, and obtained the optimal (Al+Fe)/Si, OH/(Al+Fe) molar ratio in reducing the turbidity and COD. Thus, study on introducing  $\text{SiO}_3^{2-}$  or  $\text{PO}_4^{3-}$  into  $\text{Fe}^{3+}$ ,  $\text{Al}^{3+}$  has drawn much attention. Whereas, much of the information

about poly-ferric-aluminum-silicate-sulfate's properties is undiscovered, the purpose of this work is to give a detailed study on the characterization and coagulation–flocculation performance of PFASS to fulfill the gap in the literature. Meanwhile, the abilities of adsorption–charge neutralization and adsorption–bridge are carefully researched.

In this study, the composite coagulant poly-ferric-aluminum-silicate-sulfate was synthesized by introducing PS and  $\text{Al}_2(\text{SO}_4)_3$  into  $\text{Fe}_2(\text{SO}_4)_3$  under different Si/[Al+Fe], Al/Fe, OH/[Al+Fe], and aging time, single-factor method was used to examine the parameters which influenced coagulation–flocculation behavior by municipal wastewater treatment. In addition, Fourier transformed infrared (FT-IR) spectrophotometer, X-ray diffraction (XRD), and scanning electron microscopy (SEM) was used to observe the possible chemical bonds and the morphology of PFASS. Furthermore, by analyzing the zeta potential changes in different coagulation conditions, the main coagulation mechanism of coagulation process is discussed.

## 2. Materials and methods

### 2.1. Material

All used reagents were analytically pure chemicals except  $\text{FeSO}_4 \cdot 7\text{H}_2\text{O}$  (CAS: 7720-78-7) and water glass (CAS: 1344-09-8), which was of technical grade, and the concentration of active ingredients were 89 and 26% (Calculated as  $\text{SiO}_2$ ), respectively. Deionized water with conductivity lower than 0.5  $\mu\text{S}/\text{cm}$  was used to prepare all the solutions, which were made carbonate free by boiling. The other reagents used in this study include aluminum sulfate ( $\text{Al}_2(\text{SO}_4)_3 \cdot 18\text{H}_2\text{O}$ , CAS:10043-01-3), sodium chlorate ( $\text{NaClO}_4$ , CAS:7601-89-0), sodium bicarbonate ( $\text{NaHCO}_3$ , CAS:144-55-8), e.g.

### 2.2. Preparation of coagulants

The preparation method of PSiC includes the following two steps:

#### 2.2.1. Preparation of polysilicic acid solution

Water glass solution was placed in a plastic beaker and diluted to a concentration of 3.5–4.0% (w( $\text{SiO}_2$ )) with deionized water. The diluted water glass was introduced slowly (5.0 ml/min) into  $\text{H}_2\text{SO}_4$  solution (20%) at 20°C under magnetic stirring, then regulate the value to 4.0–4.5, and followed by 60 min of polymerization to obtain a PS solution. After that the pH was decreased to 2, and added into ferric sulfate solutions (Section 2.2.2) as soon as possible.

It is worth noting that the polymerization rate of silica is relatively quick between pH 6.5 and 8.5, the initial pH of the diluted water glass solution was around 12.0. So the dosing sequence should add sodium silicate to the sulfuric acid, pH kept under 5 as well.

### 2.2.2. Preparation of coagulants

First, according to different Fe/Al molar ratios, exactly  $\text{FeSO}_4 \cdot 7\text{H}_2\text{O}$  was dissolved in  $\text{H}_2\text{SO}_4$  solution (20%, industry grade), then placed in a thermostatic water bath at a temperature range of  $80^\circ\text{C}$  under slow stirring to obtain a homogeneous  $\text{FeSO}_4$  mixture solution. After that  $\text{NaClO}_3$  solution (50%) was added slowly into reaction system as oxidant, after 10 min, a certain amount of  $\text{Al}_2(\text{SO}_4)_3 \cdot 18\text{H}_2\text{O}$  was put into mixture solution according to Al/Fe between 6:4 and 1:9.

Besides, various amounts of poly silicic acid solution (Section 2.2.1) were added at a flow rate of 5.0 mL/min into the ferric aluminum solution at  $80^\circ\text{C}$  under stirring to obtain different Si/(Fe+Al) molar ratios. Furthermore, alkalinity degree of the product was adjusted by adding  $\text{NaHCO}_3$  power to obtain the desired  $r$  value ( $r = \text{OH}/\text{Fe}$  molar ratio). At last, after stirring for 60 min, a brown–yellow liquid coagulant PFASS was obtained. The degree of product polymerization increased after aging for more than 24 h at room temperature.

### 2.3. Characterization of PFASS

Samples of PFS, PFAS, PFASS-0.4, PFASS-1.0 (PFASS-0.4, PFASS-1.0 represent the Si/(Fe+Al) = 0.4, 1.0, respectively) were placed in beakers and dried in a vacuum at  $50^\circ\text{C}$  for several days, mortar and 400 mesh screen was used to grind the drying coagulate for further characterization.

#### 2.3.1. FT-infrared spectroscopy

FTIR spectra were measured by infrared spectra Prestiger-21 from Japan in the range of  $4,000\text{--}400\text{ cm}^{-1}$ , the sample pellet was prepared by mixing with potassium bromide (KBr) for analysis.

#### 2.3.2. XRD spectroscopy

The coagulant crystalline phases were determined by characterizing the produced sample powders in XRD, using a D/Max-3C X-ray diffractometer with Cu K radiation in the range of  $5^\circ\text{--}75^\circ$  ( $2\theta$ ) at a scan rate of  $4^\circ/\text{min}$ .

#### 2.3.3. Scanning electron microscopy

The morphology of the coagulants was observed by SEM supplied by Vega II LMU from Czech Republic.

### 2.4. Coagulation experiments (jar test)

The wastewater samples used in experiment were taken from sewage outfall of Chongqing University. The large particles of the raw water were removed by graticule mesh, the pH, turbidity, COD, and zeta potential of colloids were 7.8–8.5, 110–150 NTU, 250–400, and  $-19.5\text{ mV}$ , respectively. The initial pH of the wastewater was adjusted to the set value using 0.5 mol/L HCl and NaOH.

The coagulation experiments were performed using a jar test apparatus with six paddles (ZR4-6, Zhongrun Water Industry Technology Development Co. Ltd., China) at room temperature. 500 ml of raw water was placed in a beaker, a certain of coagulant was transferred into a beaker and stirred rapidly at 250 rpm for 60 s, followed by a slow floc-increase phase at a speed of 30 rpm for 10 min, and sedimentation for 30 min. After that a supernatant sample 3.0 cm below the surface of test wastewater was extracted for turbidity and COD measurement, which were achieved by HACH 2100Q, Potassium dichromate method (GB 11984-89, China), respectively. The zeta potential of colloid was determined immediately after the rapid mixing phase. The volume of flocs precipitated in the bottom of the beaker was measured by graduated cylinder after coagulation–flocculation process. Coagulation experiments were run in triplicate, and the results were the average of two most similar in three values.

## 3. Results and discussion

### 3.1. FTIR spectra analysis

The main chemical bonds and its variation in coagulant can be drawn by analyzing the coagulant chemical structure, next compared with the results of coagulation beaker experiment can predict the optimal preparation of coagulant. By examination, the FT-IR characteristic peaks of PFS, PFAS, PFASS-0.4, PFASS-1.0, in the range of  $4,000\text{--}400\text{ cm}^{-1}$ , compared with the corresponding chemical bonds, the possible chemical bonds and their variability with the varies of element and their content can be identified. Fig. 1 shows the FT-IR spectroscopy for PFS, PAFS, PAFS-0.4, PAFS-1.0, respectively.

As shown in Fig. 1, the four coagulant spectra exhibit a broad absorption peak in the range of  $3,450\text{--}3,350\text{ cm}^{-1}$  ( $3,415\text{ cm}^{-1}$  for PFS,  $3,388\text{ cm}^{-1}$  for

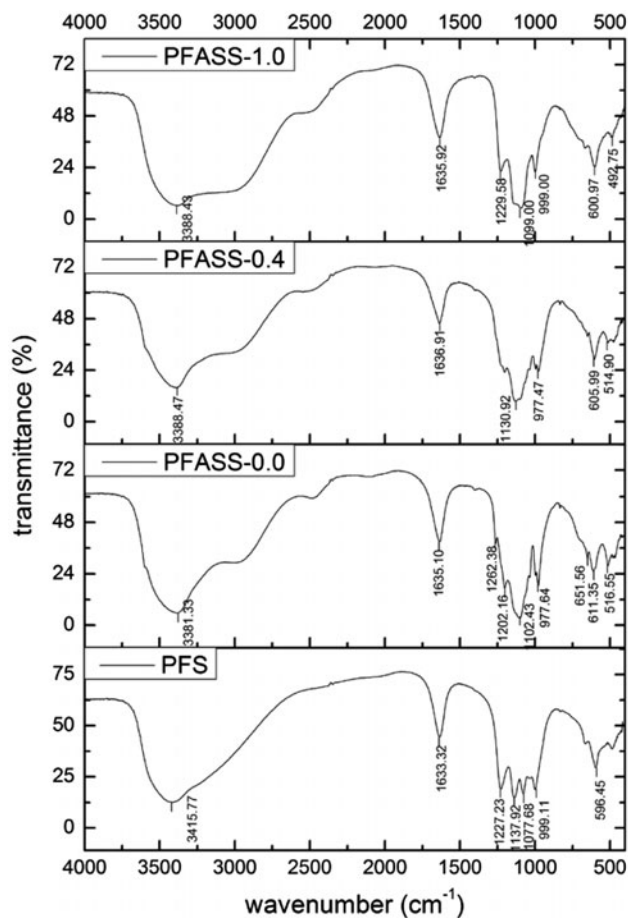


Fig. 1. The FT-IR spectra of PFS, PAFS, PAFS-0.4, and PAFS-1.0.

PAFS-0.0,  $3388\text{ cm}^{-1}$  for PAFS-0.4 and PAFS-1.0) and  $1637\text{--}1633\text{ cm}^{-1}$ , which can be associated with the stretching vibration of  $\text{--OH}$  and with the bending vibration of water absorbed, this can be regarded as the four coagulants contain absorbed, polymerized, and crystallized water [13,14]. Compared with the four coagulants, the intensity of peaks in PAFS-1.0 and PAFS-0.0 is stronger than PFS and PAFS-0.4, which reveals that PAFS-1.0 and PAFS-0.0 consist in more  $\text{--OH}$ , and are mainly associated in the form of free radicals.

While PFS and PAFS-0.4 contain more chelate  $\text{--OH}$ . For coagulant,  $\text{--OH}$  group is one of important factors affect the coagulant efficiency. However, near the wavelength of  $1400$  and  $2450\text{ cm}^{-1}$ , a weak absorption peaks appear on PAFS-0.0, PAFS-0.4, PAFS-1.0, while it did not exhibit in the PFS and it was a significant difference in the spectra of PFS and others, so it can deduce that the absorption peaks of  $1400$  and  $2450\text{ cm}^{-1}$  should be assigned to  $\text{Al--O--Al}$  bonds stretching and bending vibrations. Similarly, the peaks

around  $500\text{ cm}^{-1}$  could be assigned to the stretch vibration of  $\text{Al--O}$  bonds, and with the increase of  $\text{Si}/(\text{Fe}+\text{Al})$  from 0 to 1, the intensity of both peaks decreases [11,15,16]. Simultaneously, in the range of  $1099\text{--}1137\text{ cm}^{-1}$ , there are several absorption peaks in four products, which can be attributed to the asymmetric stretching vibration of  $\text{Fe--OH--Fe}$  or  $\text{Al--OH--Al}$ . Furthermore, the spectroscopy also showed characteristic peaks between  $977$  and  $999\text{ cm}^{-1}$ , which are assigned to the bending vibration of  $\text{Si--O--Al}$  or  $\text{Si--O--Fe}$  bonds. While the absorption peak in the range of  $596\text{--}611\text{ cm}^{-1}$  is the characteristic frequency for  $\text{Fe--O}$  groups. From Fig. 1, the conclusion can be drawn that with the difference of  $\text{Si}/(\text{Fe}+\text{Al})$  molar ratio, the quantity and species of chemical bonds in coagulant will change [17].

### 3.2. XRD analysis

The possible chemical bonds of coagulant can be exhibited by FT-IR spectrum; furthermore, the compounds or phases of product were identified using the X-ray powder diffraction. Here, take the powder of four coagulants as the analysis sample. Fig. 2 shows the XRD pattern of PFS, PAFS, PAFS-0.4, PAFS-1.0, respectively.

Fig. 2 shows the XRD pattern of PFS, PAFS, PAFS-0.4 with  $\text{Si}/(\text{Fe}+\text{Al})$  molar ratio of 0.4, and PAFS-1.0 with  $\text{Si}/(\text{Fe}+\text{Al})$  molar ratio of 1.0. According to the jade6.0 analysis, the four XRD showed that the same major phase was  $\text{Fe}^{3+}_2(\text{OH})_2(\text{SO}_4)_2\cdot 7\text{H}_2\text{O}$  at  $2\theta$  of  $12.8^\circ$ ,  $21.1^\circ$ ,  $28^\circ$ ,  $32.4^\circ$ ,  $33.0^\circ$ , and  $34.03^\circ$ , which were similar to the crystal structure of  $\text{Fe}_{0.2}(\text{Fe,Ti})_{0.6}(\text{SO}_4)(\text{OH})_{0.8}\cdot 0.2\text{H}_2\text{O}$ , these iron sulfate salts were nonstoichiometric compounds, their basic structure did not easily change with a slight change in the composition. Diffractive crystals spectra showed that the peak of  $\text{Fe}_2(\text{SO}_4)_3$ ,  $\text{Al}_2(\text{SO}_4)_3$ ,  $\text{Fe}_2\text{O}_3$ ,  $\text{Al}_2\text{O}_3$ ,  $\text{Fe}(\text{OH})_3$ ,  $\text{Al}(\text{OH})_3$ ,  $\text{Fe}_3\text{O}_4$ , and  $\text{SiO}_2$  is weak or barely observed. Some strong intensity peaks occurred at  $2\theta = 21^\circ$ ,  $24^\circ$ ,  $28^\circ$  for PFS;  $24.28^\circ$  for PAFS-0.0;  $21^\circ$ ,  $24^\circ$ ,  $29^\circ$  for PAFS-0.4;  $23.1^\circ$ ,  $53.4^\circ$  for PAFS-1.0, however, when compared to the XRD card, the peak represent a new compound or matter which did not have standard molecular formula, respectively. The XRD at  $2\theta = 11.4^\circ$ ,  $18.2^\circ$ ,  $23.8^\circ$  is the characteristic peak of  $\text{Al}_2\text{SO}_4(\text{OH})_4\cdot 7\text{H}_2\text{O}$ , which is absent in PFS. The results demonstrated that some polymerization and conformation have appeared to synthesize complex compounds of Fe, Al, Si, and other ions, rather than a simple mixture of the raw materials [18]. Compared with four diffractions, PFS, PAFS-0.0, PAFS-0.4 presented numbers of single, sharp, intense, and well-recognizable peaks, which were the crystalline structure of product, and in these

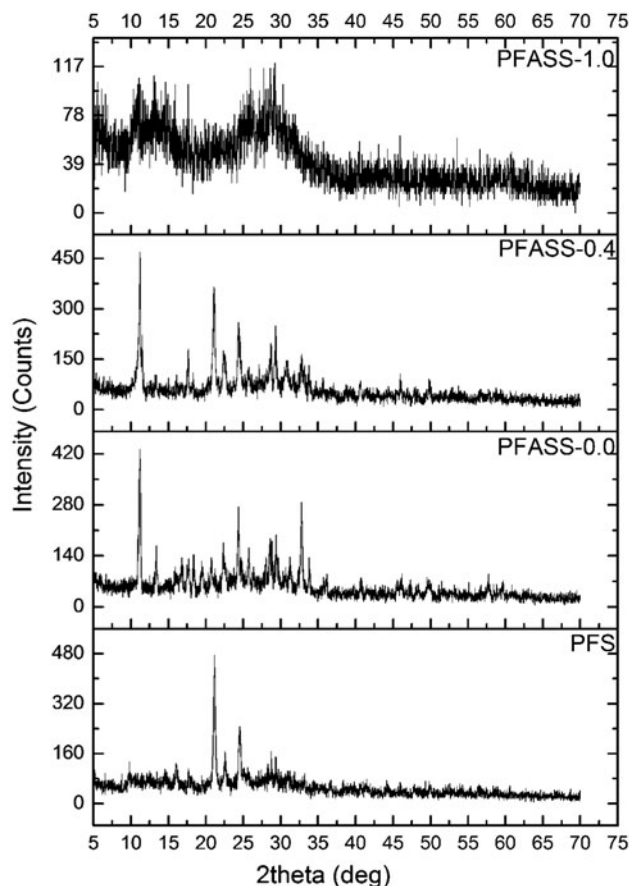


Fig. 2. The XRD pattern of PFS, PAFS, PAFS-0.4, and PAFS-1.0.

products, very little evident amorphous phase can be recognized. Whereas, for PFASS-1.0, only presents a rather broad, low intense, and not clearly recognizable peaks, and the noise produced is obvious higher than other three, which demonstrated that an amorphous phase is predominant in PFASS-1.0. The results can be attributed to that higher proportion of Fe prone to forming the crystalline phase, while larger amorphous structure was more likely to appear in high concentrations of Si, and the conclusion is consistent with Moussas e.g. [19]. Furthermore, under optimum conditions (PFASS-0.4), there were several new weak diffraction peaks, the result was ascribed to the formation of new compounds, which may in favor of the optimal coagulation effect, and the specific compounds which conducted to the good coagulation can be discussed in the future studies.

### 3.3. SEM analysis

The possible chemical bond and the phase structures of the four composite coagulants were

characterized by the FT-IR and XRD, respectively. Next, the morphology of PFS and PFASS with different Si/(Fe+Al) molar ratio observed by the SEM was investigated in the following text. Fig. 3 shows the morphology of the four coagulants in the size of 50  $\mu\text{m}$ .

Fig. 3 shows that the microstructure of four coagulants were in substantial agreement, they were obviously random crystal particles with different sizes. But with the presence of Al or Si, some apparently changes happened in their structure microscopy. Compared with four morphologies, the microparticles of PFS were small and loose, while the particles of PFASS-1.0 were spherical larger particles. It should be noted that in process of coagulation, the short-chain-like and less-branchy inorganic-inorganic hybrid material are a less favorable structure, while a multi-branched structure and fractal dimension may be the desired microstructure [20]. The reason for microparticles of PFS is that low polymerization degree lead to low morphological structure, while the reason for PFASS-1.0 is that too much  $\text{SiO}_3^{2+}$  was introduced in PFAS, due to the result of the silica gel, three-dimensional spherical structure was formed, thus, reduced the flocculation efficiency. In PFASS-0.0 and PFASS-0.4, branched structure with compact gel network structure can be observed, and an erect, curl-slice structure appeared in PFASS-0.4, which was more favorable to coagulant colloidal particles and form bridge-aggregation among flocs.

### 3.4. Effect of Si/(Fe+Al) on coagulation performance and Predominate mechanism in coagulation/flocculation process

In order to evaluate the effects of Si/(Fe+Al) on the efficiency of coagulation, a series of coagulation experiments were conducted by treating domestic sewage in terms of  $\zeta$ -potential values, removal rate of turbidity, and COD. According to the experiment results and combined with the previously relevant studies, the main coagulation/flocculation mechanisms in the impurity removal in wastewater are discussed, some new findings and conclusions will be listed at last.

Fig. 4 exhibits the comparative coagulation performance of PFASS with different Si/(Fe+Al) molar ratio. As illustrated in Fig. 4(a), the efficiency of turbidity removal increased markedly with the addition of coagulant below 1.0 mmol/L (note as Fe moles, the same below), whereas, when the dosage was above 1 mmol/L, the increase in turbidity removal is not obvious. In this experiment, the raw turbidity and COD of wastewater were 128 NTU and 328, respectively. It was characterized by high turbidity and

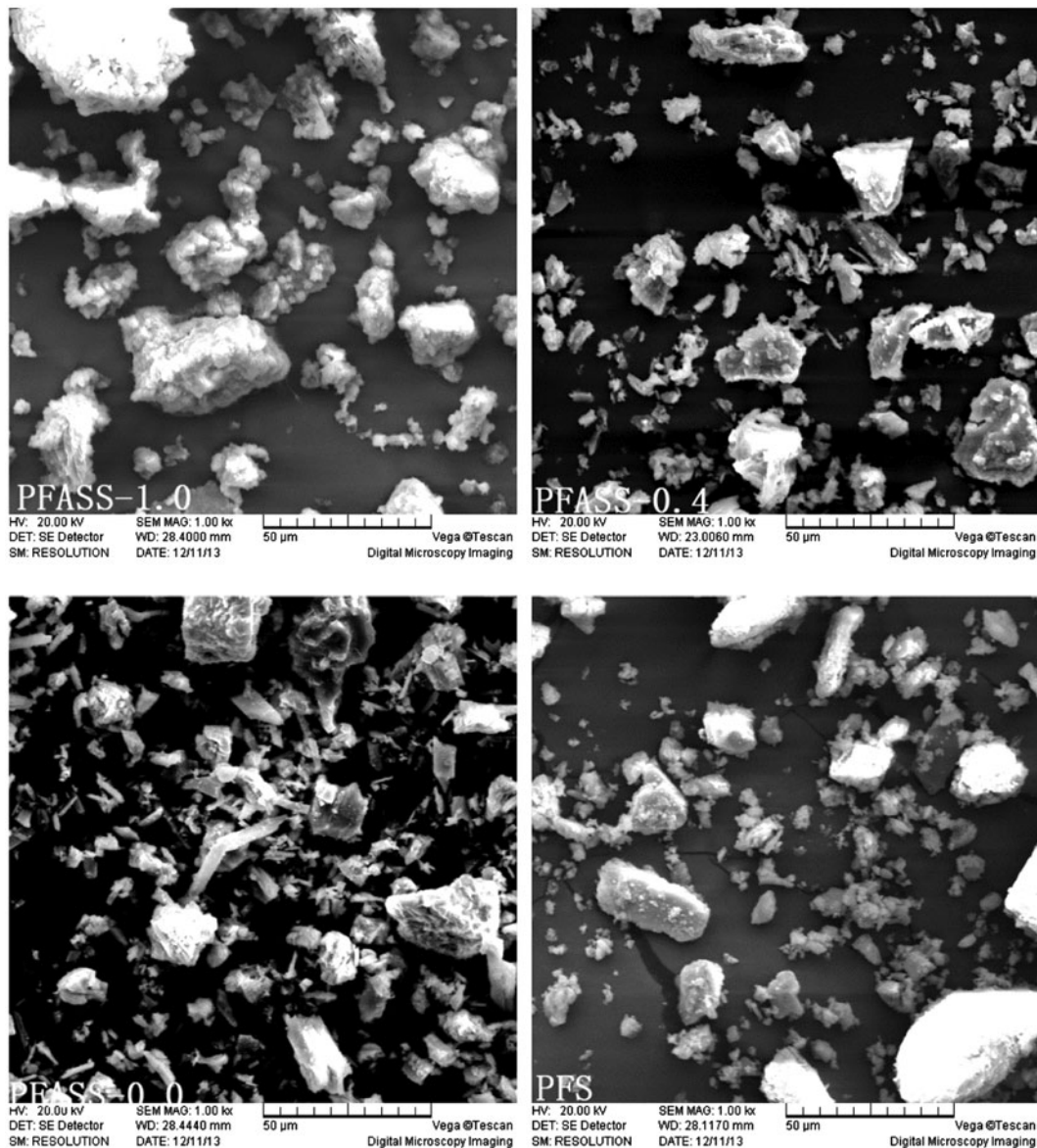


Fig. 3. The morphology of PFS, PAFS, PAFS-0.4, and PAFS-1.0.

COD and a mass of colloidal particles suspended in the solution. Moreover, the effect of six Si/(Fe+Al) molar ratio coagulant on turbidity removal was minor, which can be explained that SiO<sub>2</sub> in coagulant did not exert predominant role in coagulation/flocculation process. Compared with six Si/(Fe+Al) molar ratio coagulant, PFASS-0.4 and PFASS-0.6 exert superior coagulation performance, even in higher coagulate dose. While the PFASS-0.0 and PFASS-0.2 decreased in turbidity remove efficiency. It is of great significance to mention that a wide dosing window is convenient to actual water/wastewater treatment, for the water quality of natural body is varies all the time

[21]. The phenomenon of wide flocculants window maybe due to the presence of anionic SiO<sub>2</sub> react with Fe, formed the bond structure as –Si–Fe–, Fe–O–Si, etc., which on one hand, decrease the  $\zeta$ -potential values of Fe-coagulant, increase the molecular aggregation degree on the other hand.

Fig. 4(c) presents the change of  $\zeta$ -potential values as a continuation of coagulant dosing, as illustrated from the figure, the zeta potential of colloid particles increased homogeneous with the adding of coagulant, but all of them were blow 0 mv. Compared with six coagulants, as the concentration of SiO<sub>2</sub> gradually increases within the composition of coagulants, the

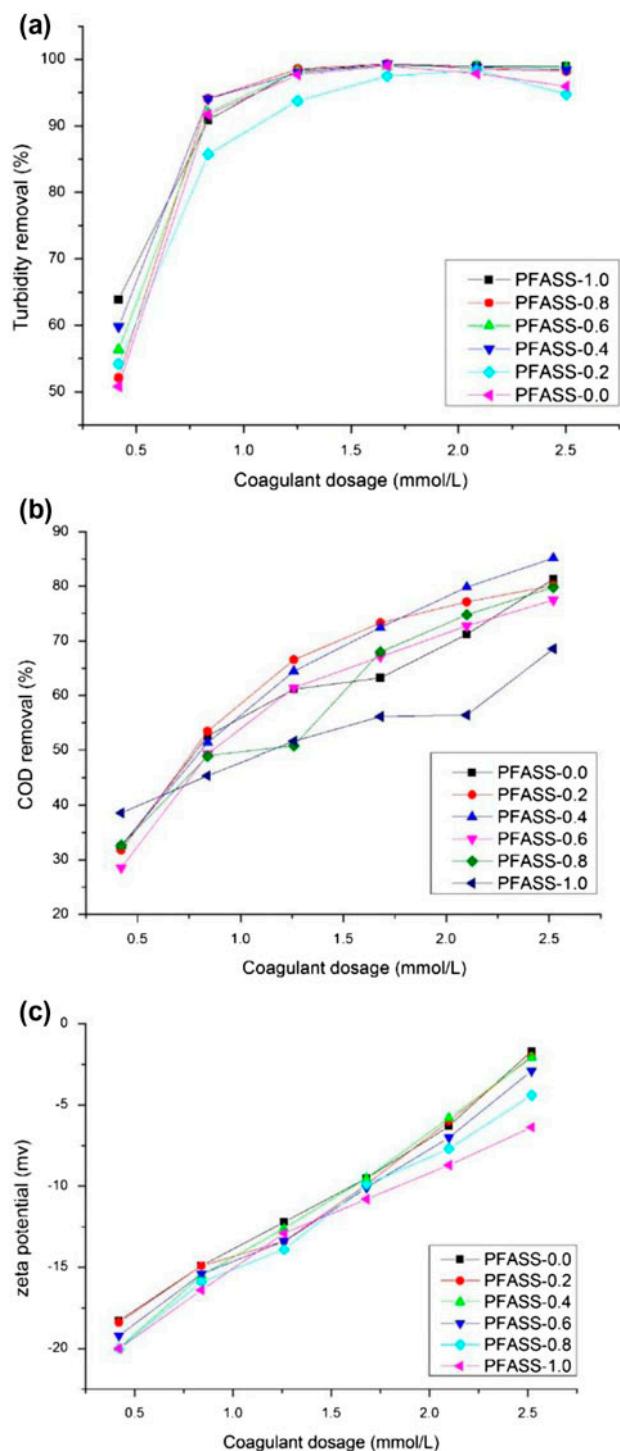


Fig. 4. The effects of Si/(Fe+Al) on removal efficiency of turbidity, COD, and the change of  $\zeta$ -potential values. (a) The effects of Si/(Fe+Al) on turbidity removal; (b) the effects of Si/(Fe+Al) on COD removal; (c) the effects of Si/(Fe+Al) on the change of  $\zeta$ -potential values).

observed reduction of zeta potential of these particles becomes lower, which can be explained that anionic

$\text{SiO}_2$  decreased the charge neutralization abilities of coagulant. Furthermore, at higher dosing, even the turbidity removal efficiency in PFASS-0.0 and PFASS-0.2 appeared deteriorating phenomenon, zeta potential exhibit below the isoelectric point as well [21]. Through which the conclusion can be drawn that charge neutralization mechanism is not the single factor favors the destabilization of particles, so, the result demonstrates the limitation of the zeta potential method, and which cannot be used to evaluate the optimal dosage of PFASS.

Based on the two figures above, the result in Fig. 4(a) can be attributed to as soon as Fe-coagulant is added into suspension liquid, the quickly hydrolysis of Fe formed large and high cationic charge molecules, the anionic character of the suspended characterized could be absorbed into iron polymeric species due to the adsorption/charge neutralization mechanism, thus formed the original small flocs. At higher particle concentration, countless particles may collide with several others, promoted the formation of large flocs, and it should be noted that in these phases, the adsorption/bridge formation mechanism is predominant which facilitates the formation of bridges between adjacent particles. Due to mass of colloids adsorbed onto flocs, high-anion properties and large size characterize the characterized microflocs or large particles, further addition of coagulant, predominates adsorption and charge neutralization mechanism until the superfluous dose leads to the appearing of isoelectric point and coagulant's performance began to deteriorate (2.5 mmol/L).

Fig. 4(b) shows the COD removal efficiency of PFASS with the increment of adding dosage. Being different from turbidity, the value of COD keeps decreasing along with the addition of coagulant in the dose range of 0.5–2.5 mmol/L. However, it is of great importance to mention that the removal efficiency of COD can reach 55% around in the dosing 1.0 mmol/L, while adding more coagulant to 2.5 mmol/L, the corresponding removal rate only increased 25–30%. Compared to Fig. 4(a), turbidity removed above 90% at the dose of 1.0 mmol/L. In suspension liquid, especially in domestic wastewater, substance can be divided into suspended/colloidal particles and dissolved particles according to particle size spectrum [22], while suspended particles favor the formation of the flocs and precipitation in the coagulation/flocculation process. Overwhelming majority of NTU and part of COD is caused by suspended particles in domestic wastewater, so the figure drawn from the experiment can be explained that as soon as coagulant dosing into water sample, the colloidal particles destabilized and sedimentate even in lower coagulant dose. The portion of COD contained in dissolved particles was removed

only by adding higher dosing, even a fraction of COD cannot be eliminated by the means of coagulation/flocculation process. The difference in COD removal with six Si/(Fe+Al) molar ratio coagulants was also distinctly displayed in Fig. 4(b), from which the result can be obtained that Si/(Fe+Al)=0.2, 0.4, 0.6 reveals better flocculation performance than others, while Si/(Fe+Al)=1.0 exhibit worst. The results can be illustrated that the introduction of silicic has combined with Fe(III) and its hydrolysis products by Fe–O–Si bonds to form hydroxy ferrous silicate species [23], which strengthens the abilities of adsorption/bridge formation and favors the formation of the large flocs in the coagulation/flocculation tests. While an excess of silicic, especially Si/(Fe+Al)=1.0 or more, the COD removal efficiency deteriorates, the result possibly dues to two reasons: I. Overdose of silicic lowered the value of  $\zeta$ -potential in coagulant, which further lessening the destabilization ability of coagulation reagents, II. Some previous relevant studies suggested that the presence of silicic does not favor the removal of natural organic matter in raw [24]. In conclusion, it is of importance that the proper Si/(Fe+Al) molar ratio is conducive to removal of turbidity and COD. Combined with Fig. 4(a) and (c), the Si/(Fe+Al)=0.4 is optimal in process of experiments.

### 3.5. Effect of Al/Fe on coagulation performance

Aluminum and ferric salts are extremely versatile coagulants in the treatment of drinking water and wastewater around the world for their good flocculation performance. However, some unavoidable limitations of traditional mono-Al or mono-Fe salts have raised great concerns such as, the residual aluminum of treated water by Al-coagulant may pose a threat to human health and the environment, while serious chroma and strong corrosive may be caused by Fe-coagulant. Therefore, a complex coagulant composed of iron and aluminum components in proper Al/Fe molar ratio is ideal, as it possesses the advantages of coagulants instead of their disadvantages [18]. Furthermore, the complex coagulant can reduce the effluent concentration of aluminum effectively. Fig. 5 illustrates the effect of Al/Fe molar ratio on turbidity and COD removal efficiency.

Fig. 5 exhibits the effect of Al/Fe molar ratio on turbidity and COD removal efficiency. It showed that there is a sharp increase in the turbidity and COD removal efficiency as the adding dose increased from 0 to 1.5 mmol/L. Fixing the amount of coagulant dosing at 1.5 mmol/L, the influence sequence of Al/Fe molar ratio on turbidity removal efficiency in

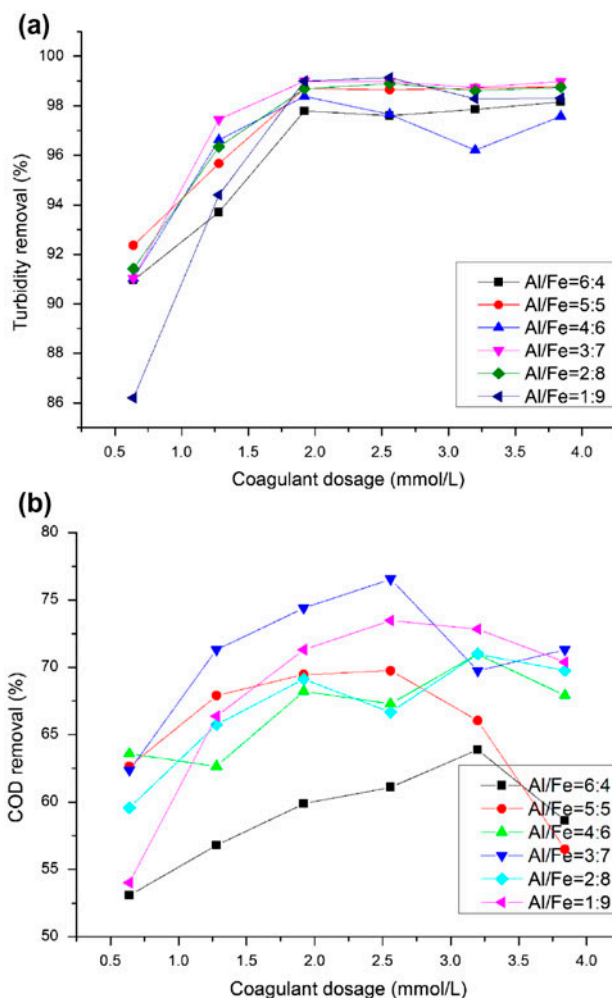


Fig. 5. The effects of Al/Fe on turbidity and COD removal efficiency. (a) The effects of Al/Fe on turbidity removal; (b) the effects of Al/Fe on COD removal).

flocculation performance as shown in Fig. 5(a) is  $3/7 > 4/6 > 2/8 > 5/5 > 1/9 > 6/4$ , which means that the turbidity removal efficiency increases with the Al/Fe molar ratio increased from 1:9 to 3:7, while for Al/Fe molar ratio greater than 3:7, the performance brought out a slight decrease. The same or roughly similar conclusion can be drawn along with each applied coagulant dosage in Fig. 5(a). However, the difference of removal efficiency is within 5% among six coagulants. In Fig. 5(b), Al/Fe molar ratio of 3/7, 5/5, and 1/9 exhibited superior flocculation performance in COD removal efficiency, while Al/Fe=3/7 manifests broader flocculation window than the others. Above all, the optimal Al/Fe molar ratio drawn from the studies is Al/Fe=3/7, which is favorable in turbidity and COD removal.



### 3.6. Effect of $\text{OH}/(\text{Fe}+\text{Al})$ and aging time on coagulation performance

Hydroxyl degrees play a vital role in the process of product preparation. During the  $\text{OH}^-$  addition process, several hydrolysis and polymerization reactions may occur, resulting in the formation of various iron or aluminum species [25]. In the lower  $\text{OH}^-$  addition, on one hand, insufficiency polymerization reactions caused absence of polymeric species and lower molecular weight; in the pH range around 1, accelerating gel effect of silicic acid would deteriorate stability of coagulate on the other hand [26]. While in higher  $\text{OH}^-$  concentration, the presence of  $\text{Fe}(\text{OH})_3$  would decrease the coagulation efficiency. Fig. 6 shows the effects of  $\text{OH}/(\text{Fe}+\text{Al})$  and aging time on coagulation performance at coagulant dosing 2.0 mmol/L.

The data obtained from experiment are presented in Fig. 6. Fig. 6(a) and (b) show that the gap in turbidity and COD removal efficiency between six  $\text{OH}/(\text{Fe}+\text{Al})$  was small, which are 98.4–99.4% and 69–78% for turbidity and COD removal, respectively. But some differences still can be identified in full range as well. Lower or higher  $\text{OH}/(\text{Fe}+\text{Al})$  exhibited poorer coagulation performance, while in aging time at  $3 \times 24$  h,  $\text{OH}/(\text{Fe}+\text{Al}) = 0.6$  also performed worse removal efficiency. Whereas, Fig. 6(c) shows that when the aging time is 15 d and  $\text{OH}/(\text{Fe}+\text{Al})$  above 0.4, the coagulation performance decreased with the increasing of  $\text{OH}^-$  concentration.

The appearance of the product changed with  $\text{OH}/(\text{Fe}+\text{Al})$  and aging time. The pH of coagulant solution is around 1 when the  $\text{OH}/(\text{Fe}+\text{Al}) = 0.2$  or lower, which accelerate the gel effect of silicic acid. Furthermore, lower  $\text{OH}/(\text{Fe}+\text{Al})$  is inconvenient to the polymerization of  $\text{Fe}(\text{III})$  species, leading to lower degree of polymerization [27,28]. However, at higher  $\text{OH}/(\text{Fe}+\text{Al})$ , a higher basicity accelerates the arise of  $\text{Fe}(\text{OH})_3$  via a series of hydrolysis processes, and the appearance of yellow iron hydroxide precipitation reduced the coagulation efficiency in coagulation/flocculation process [29]. Therefore, both too low or too high  $\text{OH}/(\text{Fe}+\text{Al})$  would result in negative effects on coagulation performance. In this study, comprehensive comparison of the influence of  $\text{OH}/(\text{Fe}+\text{Al})$  in coagulation efficiency, the proper  $\text{OH}/(\text{Fe}+\text{Al})$  is 0.3.

### 3.7. Effect of $\text{Si}/(\text{Fe}+\text{Al})$ on the sludge production

Sludge production and sludge moisture content is a great important index in water/wastewater treatment plant, for the treatment of huge production of waste sludge account for the very great proportion in daily operating costs. Fig. 7 shows the effect of

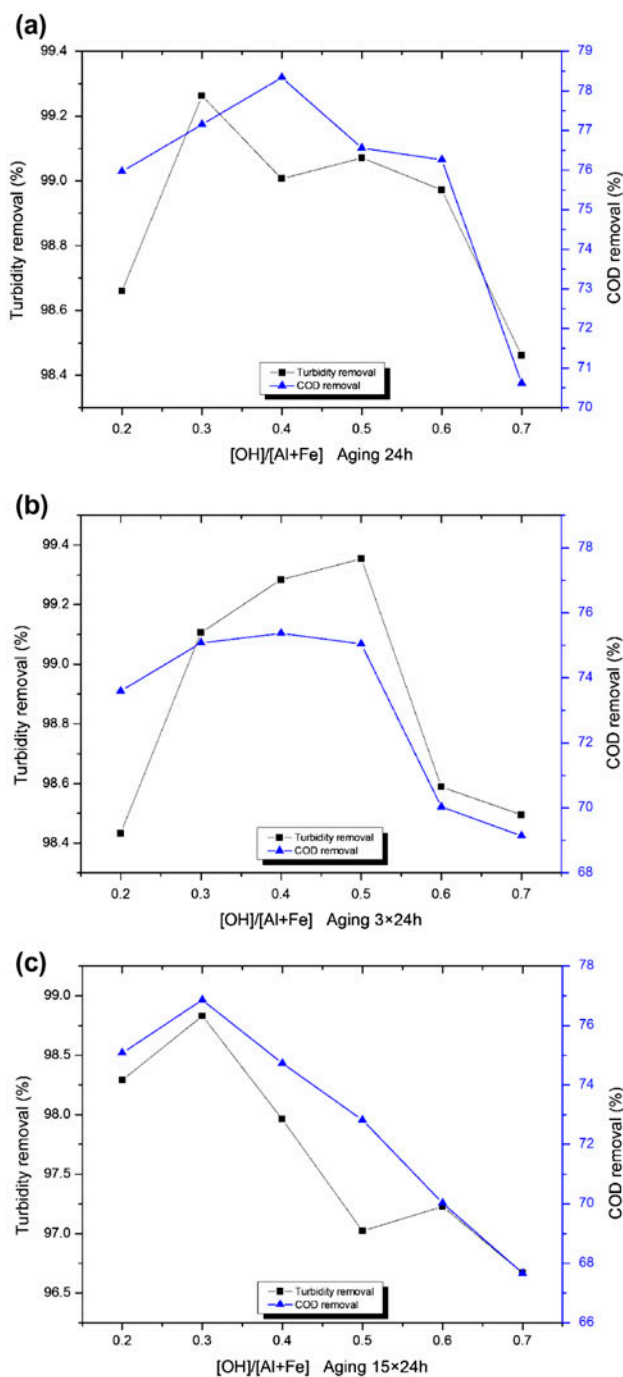


Fig. 6. The effects of  $\text{OH}/(\text{Fe}+\text{Al})$  and aging time on coagulation performance. (a) The effects of  $\text{OH}/(\text{Fe}+\text{Al})$  on turbidity removal at aging time 24 h; (b) the effects of  $\text{OH}/(\text{Fe}+\text{Al})$  on turbidity removal at aging time  $3 \times 24$  h; (c) the effects of  $\text{OH}/(\text{Fe}+\text{Al})$  on turbidity removal at aging time  $15 \times 24$  h.

coagulants with different  $\text{Si}/(\text{Fe}+\text{Al})$  molar ratio on the sludge production. The graph illustrated that the coagulants without silicic acid produced maximum

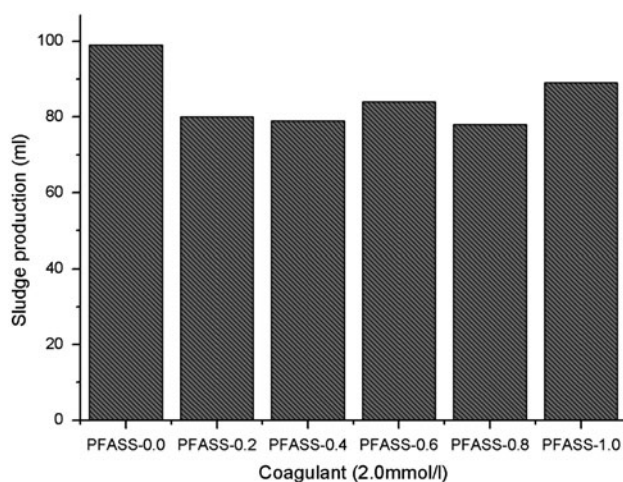


Fig. 7. The effect of Si/(Fe+Al) on the sludge production.

sludge volume at the same jar test experiment conditions. The results can be interpreted as the introduction of silica acid into coagulant enhanced the adsorption, entrapment, and interparticle bridging performance of coagulant, which is favorable for the formation of more compact and lower moisture content flocs in coagulation–flocculation process, and the research conclusion is consistent with previous research results [23]. Whereas, the addition of supplementary silicic acid decreased the coagulation performance, result in low impurity removal rate and higher sludge volume. Overall, consider the effect of Si/(Al+Fe) on coagulation–flocculation efficiency, Si/(Al+Fe)=0.2 and 0.4 showed better integrated coagulation performance.

Economic performance is of paramount significance in water/wastewater treatment process. The conventional coagulant used in domestic wastewater treatment process is PAC, while the dosage of PFASS is much less than PAC at the same turbidity and COD removal efficiency, which is beneficial to economic performance in water/wastewater plant.

#### 4. Conclusions

In this research, a modified coagulation reagent poly-ferric-aluminum-silicate -sulfate for wastewater treatment was prepared and detailed studied. The main conclusions withdrawn from this analysis results are as follows:

- (1) FTIR spectra result shows that new chemical bonds as Al–O, Si–O–Fe, Si–O–Al were found in compound, and with the difference of Si/(Fe+Al) molar ratio, the quantity and

species of chemical bonds in coagulant will change. Meanwhile, XRD analysis result exhibits the major phase is  $\text{Fe}_2^{3+}(\text{OH})_2(\text{SO}_4)_2 \cdot 7\text{H}_2\text{O}$  at six Si/(Fe+Al) molar ratio, and the diffraction peaks of PFASS-0.4 show that some new formed compounds may favor the performance of coagulation/coagulation process. SEM analysis result demonstrates that PFASS-0.4 was convenient to absorb colloidal particles and form bridge–aggregation among flocs.

- (2) Coagulation/flocculation experiments demonstrate that the optimal synthetic proportion of coagulant in wastewater treatment is Si/(Fe+Al) = 0.4, Al/Fe = 3:7, OH/(Fe+Al) = 0.3, and the maximum treatment efficiency of turbidity and COD removal efficiency can reach 99.4, 85.6%, respectively, at the optimum coagulant dosage of 2.5 mmol/L. In addition, when the Si/(Fe+Al) molar ratio of PFASS is 0.2 and 0.4, the coagulation–flocculation process produced fewer sludge volume compared to other coagulant. The small amount composition of aluminum in coagulant can reduce the residual aluminum concentration remained in effluent effectively. The conclusion can be drawn from the experiments that at lower coagulant dosage, adsorption/bridge formation mechanism is predominant, while in higher coagulant dosage, adsorption/charge neutralization mechanism becomes more and more important. But the predominant mechanism maybe varies in different water samples.

#### Acknowledgments

The research was supported by the National Natural Science Foundation of China (Projects 21177164) and Major projects on control and rectification of water body pollution (2013ZX07312-001-03-03). The kind suggestions from the anonymous reviewers are greatly acknowledge by authors.

#### References

- [1] F. Ni, X. Peng, J. He, L. Yu, J. Zhao, Z. Luan, Preparation and characterization of composite biofloculants in comparison with dual-coagulants for the treatment of kaolin suspension, *Chem. Eng. J.* 213 (2012) 195–202.
- [2] R. Ordóñez, D. Hermosilla, N. Merayo, A. Gascó, C. Negro, Ángeles Blanco, Application of multi-barrier membrane filtration technologies to reclaim municipal wastewater for industrial use, *Sep. Purif. Rev.* 43 (2014) 263–310.
- [3] J.C. Lou, Y.S. Hsu, K.L. Hsu, M.S. Chou, J.Y. Han, Comparing the removal of perchlorate when using

- single-walled carbon nanotubes (SWCNTs) or granular activated carbon: Adsorption kinetics and thermodynamics, *J. Environ. Sci. Health. Part A Toxic/Hazard. Subst. Environ. Eng.* 49 (2014) 503–513.
- [4] W.P. Cheng, F.H. Chi, A study of coagulation mechanisms of polyferric sulfate reacting with humic acid using a fluorescence-quenching method, *Water Res.* 36 (2002) 4583–4591.
- [5] G. Zhu, H. Zheng, W. Chen, W. Fan, P. Zhang, T. Tshukudu, Preparation of a composite coagulant: Polymeric aluminum ferric sulfate (PAFS) for wastewater treatment, *Desalination* 285 (2012) 315–323.
- [6] C. Sun, Q. Yue, B. Gao, B. Cao, R. Mu, Z. Zhang, Synthesis and floc properties of polymeric ferric aluminum chloride–polydimethyl diallylammonium chloride coagulant in coagulating humic acid–kaolin synthetic water, *Chem. Eng. J.* 185–186 (2012) 29–34.
- [7] P. Jarvis, E. Sharp, M. Pidou, R. Molinder, S.A. Parsons, B. Jefferson, Comparison of coagulation performance and floc properties using a novel zirconium coagulant against traditional ferric and alum coagulants, *Water Res.* 46 (2012) 4179–4187.
- [8] P.A. Moussas, A.I. Zouboulis, Synthesis, characterization and coagulation behavior of a composite coagulation reagent by the combination of polyferric sulfate (PFS) and cationic polyelectrolyte, *Sep. Purif. Technol.* 96 (2012) 263–273.
- [9] Y. Zeng, J. Park, Characterization and coagulation performance of a novel inorganic polymer coagulant—Poly-zinc-silicate-sulfate, *Colloids Surf., A* 334 (2009) 147–154.
- [10] B.-Y. Gao, Q.-Y. Yue, Y. Wang, Coagulation performance of polyaluminum silicate chloride (PASiC) for water and wastewater treatment, *Sep. Purif. Technol.* 56 (2007) 225–230.
- [11] T. Sun, C.-H. Sun, G.-L. Zhu, X.-J. Miao, C.-C. Wu, S.-B. Lv, W.-J. Li, Preparation and coagulation performance of poly-ferric-aluminum-silicate-sulfate from fly ash, *Desalination* 268 (2011) 270–275.
- [12] R. Li, C. He, Y. He, Preparation and characterization of poly-silicic-cation coagulants by synchronous-polymerization and co-polymerization, *Chem. Eng. J.* 223 (2013) 869–874.
- [13] K. Nakamoto, *Infrared and Raman Spectra of Inorganic and Coordination Compounds*, John Wiley and Sons, New York, NY, 1978.
- [14] Y. Fu, S.-L. Yu, Y.-Z. Yu, L.-P. Qiu, B. Hui, Reaction mode between Si and Fe and evaluation of optimal species in poly-silicic-ferric coagulant, *J. Environ. Sci.* 19 (2007) 678–688.
- [15] K.E. Lee, N. Morad, T.T. Teng, B.T. Poh, Development, characterization and the application of hybrid materials in coagulation/flocculation of wastewater: A review, *Chem. Eng. J.* 203 (2012) 370–386.
- [16] G. Zhu, H. Zheng, Z. Zhang, T. Tshukudu, P. Zhang, X. Xiang, Characterization and coagulation–flocculation behavior of polymeric aluminum ferric sulfate (PAFS), *Chem. Eng. J.* 178 (2011) 50–59.
- [17] Z. Song, N. Ren, Properties and coagulation mechanisms of polyferric silicate sulfate with high concentration, *J. Environ. Sci.* 20 (2008) 129–134.
- [18] T. Sun, L.-L. Liu, L.-L. Wan, Y.-P. Zhang, Effect of silicon dose on preparation and coagulation performance of poly-ferric-aluminum-silicate-sulfate from oil shale ash, *Chem. Eng. J.* 163 (2010) 48–54.
- [19] P.A. Moussas, A.I. Zouboulis, A study on the properties and coagulation behaviour of modified inorganic polymeric coagulant—Polyferric silicate sulphate (PF5SiS), *Sep. Purif. Technol.* 63 (2008) 475–483.
- [20] Y. Fu, S. Yu, C. Han, Morphology and coagulation performance during preparation of poly-silicic-ferric (PSF) coagulant, *Chem. Eng. J.* 149 (2009) 1–10.
- [21] Z. Yang, B. Yuan, X. Huang, J. Zhou, J. Cai, H. Yang, A. Li, R. Cheng, Evaluation of the flocculation performance of carboxymethyl chitosan-graft-polyacrylamide, a novel amphoteric chemically bonded composite flocculant, *Water Res.* 46 (2012) 107–114.
- [22] A. Matilainen, M. Vepsäläinen, M. Sillanpää, Natural organic matter removal by coagulation during drinking water treatment: A review, *Adv. Colloid Interface Sci.* 159 (2010) 189–197.
- [23] B.Y. Gao, Q.Y. Yue, B.J. Wang, Y.B. Chu, Poly-aluminum-silicate-chloride (PASiC)—A new type of composite inorganic polymer coagulant, *Colloids Surf., A* 229 (2003) 121–127.
- [24] K. Konieczny, D. Szałkol, J. Płonka, M. Rajca, M. Bodzek, Coagulation—Ultrafiltration system for river water treatment, *Desalination* 240 (2009) 151–159.
- [25] A.I. Zouboulis, P.A. Moussas, F. Vasilakou, Polyferric sulphate: Preparation, characterisation and application in coagulation experiments, *J. Hazard. Mater.* 155 (2008) 459–468.
- [26] M. Dietzel, Dissolution of silicates and the stability of polysilicic aci.pdf, *Geochim. Cosmochim. Acta* 64 (2000) 3275–3281.
- [27] W.D.T. Hongxiao, Preparation and characterization of three kinds of silica, *J. Environ. Chem.* 16 (1997) 515–521.
- [28] Z. Liang, Y. Wang, Y. Zhou, H. Liu, Z. Wu, Hydrolysis and coagulation behavior of polyferric sulfate and ferric sulfate, *Water Sci. Technol.* 59 (2009) 1129–1135.
- [29] G. Lei, J. Ma, X. Guan, A. Song, Y. Cui, Effect of basicity on coagulation performance of polyferric chloride applied in eutrophicated raw water, *Desalination* 247 (2009) 518–529.